Zuerst erschienen in: Solid State Ionics 176 (2005) 1131-1143

On the Soret effect in binary nonstoichiometric oxides—kinetic demixing of cuprite in a temperature gradient

H. Timm[a], J. Janek[b,*]

[a]*Robert Bosch GmbH, D-72762 Reutlingen, Germany*
[b]*Institute of Physical Chemistry, Justus-Liebig University Giessen, Heinrich-Buff-Ring 58, D-35392 Gießen, Germany*

Abstract

The Soret effect in nonstoichiometric copper(I)-oxide (cuprite, $Cu_{2-\delta}O$) has been studied experimentally by means of non-isothermal solid state galvanic cells (thermocells) under different boundary conditions. At high temperatures and high oxygen activities, copper metal migrates down the temperature gradient and a gradient in the nonstoichiometry is established under stationary conditions. The heat of transport of copper metal is determined as $Q^*_{Cu} \approx 180$ kJ/mol at a temperature of 1000 °C and at an oxygen activity of $\log a_{O_2} = -2.95$. This result agrees with recent theoretical simulations of the heat of transport of atoms migrating via a vacancy mechanism. These predict a positive sign of the heat of transport and a considerably larger value than the activation energy for the atomic jumps.

Keywords: Soret effect; Thermodiffusion; Mixed conductors; Degradation; Diffusion

1. Introduction

Many advanced materials for high temperature applications are multi-component ionic systems, being mostly oxides for the use in e.g. fuel cells, heterogeneous catalysis or as thermal barrier coatings. Under working conditions, these materials are often exposed to external forces causing both reactions and transport within the materials. Prominent examples are electromigration or kinetic demixing in electric fields [1–5], kinetic demixing in chemical potential gradients [6–9], stress-driven segregation [10,11] or thermodiffusion ([12–20], see [21,22] for reviews).

Thermodiffusion (or -migration) denotes diffusion in a temperature gradient and is probably still the least understood process among these transport phenomena. Thus our interest in thermodiffusion is twofold: firstly, we are interested in the degree of local composition changes in a nonstoichiometric oxide in a temperature gradient from a mere technical point of view, i.e. aiming for quantitative information on the influence of temperature gradients on the homogeneity of high temperature materials. Secondly, we pursue the determination of the so-called heat of transport of mobile components in ionic solids from a more basic point of view, trying to improve the data basis for a comparison with theoretical studies and to gain a better mechanistic understanding.

As in liquids or gases, the magnitude and the direction of thermodiffusion is formally described by non-zero cross coefficients in the matrix of transport coefficients (often denoted as “Onsager coefficients”). A useful combination of diagonal and off-diagonal transport coefficients defines the so-called heat of transport Q_k^* of a mobile component k [23], being related to both the thermodiffusion coefficient and the Soret coefficient.

As a consequence of thermodiffusion, a temperature gradient drives the establishment of a concentration gradient. In the stationary state this concentration gradient depends on the boundary conditions of the inhomogeneous system. If the system is closed for matter

* Corresponding author.
E-mail address: juergen.janek@phys.chemie.uni-giessen.de (J. Janek).

exchange, we end up with zero matter fluxes, defining the so-called *Soret state*. If the system is open for exchange of components with the surrounding, non-zero matter fluxes occur and lead to a different stationary state—not being the Soret state. Provided that our system is closed, the stationary molar concentration gradient ∇c_A of a component A for the Soret state (j_A=0) can be equated as (Q_A^* denotes the reduced heat of transport or component A, μ_A and c_A represent the chemical potential and the molar concentration of A, see Section 2):

$$\nabla c_A|_{j_A=0} = -\frac{Q_A^*}{\left(\frac{\partial \mu_A}{\partial c_A}\right)_T}\frac{\nabla T}{T} \tag{1}$$

In materials with small concentration variations (i.e. deviations from stoichiometry), rather the stationary chemical potential gradient ($\nabla \mu_A$) than the concentration gradient is addressed in a Soret experiment. This is the experimental basis for the present paper, as chemical potentials can be favourably measured in galvanic cells ($\tilde{S}_A$ represents the partial molar entropy of the component A in a compound with variable composition):

$$\nabla \mu_A|_{j_A=0} = -\left(\frac{Q_A^*}{T} + \tilde{S}_A\right)\nabla T \tag{2}$$

We chose $Cu_{2-\delta}O$ as a nonstoichiometric binary compound with a narrow phase field, as it is well characterised in respect to its isothermal transport properties during the past, mainly due to its technological relevance in early semiconductor technology. The deviation δ from stoichiometry [24–26], the electronic conductivity and thermopower [28,29] and the diffusion coefficients of copper and oxygen [30–32] have been determined by various authors. At sufficiently high oxygen activities the material is a p-type semiconductor, i.e. copper vacancies and electron holes are the majority defects. Copper ions are mobile via a vacancy mechanism, and the oxygen mobility is much lower. Thus, experimental data for the heat of transport of neutral copper metal offer direct information on the vacancy heat of transport if suitable assumptions for the electronic heat of transport can be made.

In the following, we briefly recall the necessary equations for the ionic thermopower of mixed conductors, being the basis of our experiments. We pay special attention to the different possible boundary conditions during a Soret experiment–as this is often neglected in the discussion of thermodiffusion–and show that Q_{Cu}^* can be evaluated from time-dependent measurements of the ionic thermovoltage of a closed thermocell. This non-isothermal electrochemical cell is described in detail, before the experimental results and their discussion are presented.

2. Theory

2.1. Non-isothermal flux equations

The non-isothermal flux equations of mobile ions, electrons and components within the framework of linear irreversible thermodynamics, being the starting points for any transport experiment, have been presented firstly by Wagner [33]. The relations between the flux equations of defects as structure elements, ions and electrons as building units and the chemical components have been formulated for the case of a binary compound by Janek and Korte [34]. We refer to these works for details.

In order to clarify a notorious difficulty in the understanding of thermodiffusion let us consider the transport of a mobile component in a temperature gradient in some detail: a temperature gradient creates an independent driving force which adds to the driving forces like concentration gradients or an electric field. Thus, if one considers a system with mobile components k, the well known empirical Fick's law is expanded additively by this temperature gradient term (neglecting interactions between different mass fluxes, one-dimensional system):

$$j_k = c_k v_k = -c_k\left(\tilde{D}_k\frac{\nabla c_k}{c_k} + D_k^T\frac{\nabla T}{T}\right) \tag{3}$$

In Eq. (3) the chemical diffusion coefficient $\tilde{D}_k$ relates the flux j_k of component k to the molar concentration gradient ∇c_k, and the thermodiffusion coefficient D_k^T relates the flux of k to the temperature gradient ∇T. The sum of the gradient terms in the bracket can be interpreted as the velocity v_k of the mobile component k. The empirical diffusion coefficients $\tilde{D}_k$ and $\tilde{D}_k^T$ base on the same single (self) diffusion coefficient D_k. This self-diffusion coefficient is directly related to the *microscopic jump processes* of the mobile component. In the case of chemical diffusion, the self-diffusion coefficient is multiplied (or better: amplified) by the thermodynamic factor $(\partial \ln a_k/\partial \ln c_k)_T$. In the case of thermomigration the self-diffusion coefficient is multiplied by the reduced heat of transport (normalized by RT), Q_k^*/RT, as can be seen from the flux equation

$$j_k = -c_k D_k\left[\left(\frac{\partial \ln a_k}{\partial \ln c_k}\right)_T\frac{\nabla c_k}{c_k} + \frac{Q_k^*}{RT}\frac{\nabla T}{T}\right] \tag{4}$$

which is formally equivalent to the empirical Eq. (3) but is derived within linear irreversible thermodynamics, see [21]. Eq. (4) allows to estimate the flux being driven by the two forces: In practice $\nabla T/T$=0.1 cm^{-1} will be a reasonable upper limit. Assuming a temperature around 1000 K we can approximately insert $RT \approx 10^4$ J/mol. All theories on the heat of transport result in a more or less close relation to the migration enthalpy, and thus, the activation energy of the mobile species will be a reasonable estimate. A value of 10^5 J/mol represents a typical average value for oxides, leading to a value of approx. 1 cm^{-1} for the product of Q_k^*/RT and $\nabla T/T$. In contrast, the product of the thermodynamic factor

$(\partial \ln a_k/\partial \ln c_k)_T$ and $\nabla c_k/c_k$ can become much larger in nonstoichiometric compounds with narrow phase fields. Thus, chemical diffusion driven by a concentration gradient will usually be more significant than thermodiffusion.

If the chemical potential gradient is used for the description of the driving force rather than the concentration gradient, one has to be careful not to mix chemical diffusion up with thermodiffusion in the case of open systems. A temperature difference always immediately creates a chemical potential difference, determined by the entropy. Thus, a flux equation formulated in terms of the driving forces $\nabla \mu_k$ and ∇T includes the entropy of the mobile species to account for this contribution. In the case of ions and electrons in a mixed conductor the flux equations then result as [33]:

$$j_{Cu^+} = -L_{Cu^+}\left[\nabla \tilde{\mu}_{Cu^+} + \left(\tilde{S}_{Cu^+} + \frac{Q^*_{Cu^+}}{T}\right)\nabla T\right] \tag{5}$$

$$j_{e^-} = -L_{e^-}\left[\nabla \tilde{\mu}_{e^-} + \left(\tilde{S}_{e^-} + \frac{Q^*_{e^-}}{T}\right)\nabla T\right] \tag{6}$$

The sum of the partial molar entropy $\tilde{S}_k$ of a charge carrier and its heat of transport term Q^*_k/T is often defined as the so-called *transported entropy* S^*_k (often also called *entropy of transport*). We use these quantities in the following for the sake of concise equations.

2.2. Thermopower of ionic thermocells

As it has been shown in general in [33] and [35], the chemical potential gradient in mixed conductors being exposed to a temperature gradient can be measured with ionic or electronic potential probes, depending on the majority type of conduction. The resulting partial thermopowers of ions and electrons as independent charge carriers show a characteristic time relaxation upon the exposure of a mixed conductor to a temperature gradient. This relaxation is a consequence of thermal diffusion, being a slow process with a relaxation time that is determined by chemical diffusion coefficient. A composition gradient is established and changes the average thermopower. This is used in the present study for the determination of the heat of transport. As Cu_2O is a semiconductor with $t_{Cu^+} \ll t_{e^-}$, ionic probes are employed.

As shown in detail in the Appendix (see Eqs. (28)–(37)), the thermopower of the general type of ionic thermocell

$$\xrightarrow[\nabla T]{\mathrm{Pt}'(a_{O_2})|\mathrm{YSZ}'|\mathrm{Cu}_{2-\delta}\mathrm{O}|\mathrm{YSZ}''|\mathrm{Pt}''(a_{O_2})} \tag{I}$$

can be derived as:

$$\varepsilon = \frac{d\phi}{dT} = -\underbrace{\epsilon^{Pt}_{e^-}}_{\text{const.}} - \underbrace{\frac{1}{4F}S_{O_2}}_{\text{const.}} + \underbrace{\frac{1}{2F}\Theta \cdot S_{Cu_2O}}_{\text{const.}} + \underbrace{(1-\Theta)\epsilon^{YSZ}_{O^{2-}}}_{\text{const.}} + \underbrace{\Theta \cdot \epsilon^{Cu_2O}_{Cu^+}}_{\text{const.}} \tag{7}$$

In accord with Wagner, the thermopower ε is defined as the ratio of the actual thermovoltage (potential difference) between the isothermal ends of the cell and the applied temperature difference, thus the thermopower is positive if the hot end of the cell has a more positive potential than the cold end (see Fig. 1 for scheme of temperature profile along the cell).

The thermopower is determined by the sum of several contributions, being the thermopower $\epsilon^{Pt}_{e^-}$ of the platinum electrodes, the ionic thermopower $\varepsilon^{YSZ}_{O^{2-}}$ of the YSZ electrolyte, the molar entropies S_{O_2} and S_{Cu_2O} of molecular oxygen and of the compound Cu_2O, and the ionic thermopower $\epsilon^{Cu^2O}_{Cu^+}$ of the oxide sample. The parameter Θ denotes that fraction of the total temperature difference which is applied only to the cuprite sample, F denotes Faraday's constant.

$$\Theta \equiv \frac{\Delta T(\mathrm{Cu}_{2-\delta}\mathrm{O})}{\Delta T(\mathrm{YSZ}') + \Delta T(\mathrm{YSZ}'') + \Delta T(\mathrm{Cu}_{2-\delta}\mathrm{O})} \tag{8}$$

We assume that Θ is constant, i.e. we assume that the thermal conductivities of all materials are also constant. We also assume that both YSZ electrodes are symmetric and experience the same temperature difference, and that all effects are linear ($\Delta\tilde{\mu}_i(\Theta \cdot \Delta T) = \Theta \cdot \Delta\tilde{\mu}_i(\Delta T)$). We assume a negligible temperature dependence of $\varepsilon^{Pt}_{e^-}$, S_{O_2}, S_{Cu_2O} and $\epsilon^{YSZ}_{O_2^-}$ within the applied temperature interval. Only $\epsilon^{Cu_2O}_{Cu^+}$ is subject to a change with time driven by the establishment of the Soret state.

Two different boundary conditions may be applied: (a) the surfaces and interfaces of the oxide sample are closed for the exchange of oxygen with the surrounding gas phase (*closed cell*), and (b) they are open for this exchange (*open cell*). Both cells show a different change of their thermopower after establishing a temperature gradient, and the limiting cases $t \to 0$ and $t \to \infty$ will be considered: within the very beginning of a Soret experiment ($t \to 0$), the temperature gradient is usually established much faster than a composition gradient (i.e. the thermal diffusivity λ/c_p is much larger than the chemical diffusivity $\tilde{D}$). Thus, in the beginning the thermopower of the cell will correspond to a compositionally homogenous but thermally inhomogeneous oxide sample. After this initial phase the oxide starts to demix, and the thermopower $\varepsilon^{Cu_2O}_{Cu^+}$ is changing until the stationary state with a new constant thermopower is approached ($t \to \infty$). The last term in Eq. (7) has to be evaluated in order to account for these two cases. Yoo and Hwang coined the term *heat pulse experiment* [17] in order

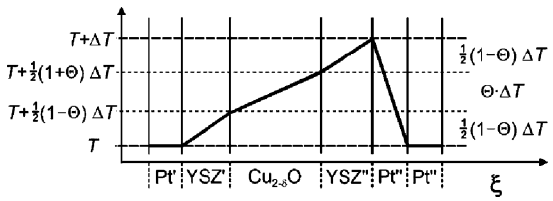

Fig. 1. Schematic temperature profile along the thermocell in Fig. 2.

to emphasize the faster establishment of the thermal stationary state than the chemical stationary state.

In order to observe this kinetic hysteresis, the chemical diffusivity has to be sufficiently smaller than the thermal diffusivity, so that the stationary temperature gradient is established much faster than the composition gradient. In the present case of copper(I)-oxide with the thermal conductivity $\lambda \approx 4$, 5J/Kms [36], the heat capacity $c_p \approx 70$ J/K mol [37] and the molar volume of V_m=23.85 cm^3/mol we estimate its value as 0.01 cm^2/s. This is much higher than the chemical diffusion coefficient $\tilde{D}_{Cu}$ which is in the orders of 10^{-5} to 10^{-4} cm^2/s [30].

2.2.1. The closed thermocell

Within the closed thermocell the oxide sample is completely isolated from the gas phase. The YSZ/oxide interface is only open for the exchange of oxygen ions.

$$\mathrm{Pt}'\,|\mathrm{YSZ}'|\mathrm{Cu}_{2-\delta}\mathrm{O}|\mathrm{YSZ}''\,|\mathrm{Pt}'' \xrightarrow[\nabla T]{} \tag{a}$$

Initial state ($t\to 0$, $\nabla\delta$=0): The initial state is characterised by coupled fluxes of ions and electrons and leads to the following result (see Eqs. (38)–(41) in Appendix):

$$\varepsilon^{(a)}_{t\to 0} = -\epsilon^{Pt}_{e^-} - \frac{1}{4F}S_{O_2} + \frac{\Theta}{2F}S_{Cu_2O} + (1-\Theta)\epsilon^{YSZ}_{O^{2-}} + \frac{\Theta}{F}\left[t_{e^-}(S^*_{e^-} - \tilde{S}_{Cu}) - t_{Cu^+}S^*_{Cu^+}\right] \tag{9}$$

The Soret state ($t\to\infty$, j_{Cu}=0): the Soret state is characterised by vanishing fluxes of ions and electrons. The thermopower of the cell can be derived as (see Eqs. (42) and (43) in Appendix):

$$\varepsilon^{(a)}_{t\to\infty} = -\epsilon^{Pt}_{e^-} - \frac{1}{4F}S_{O_2} + \frac{\Theta}{2F}\cdot S_{Cu_2O} + (1-\Theta)\epsilon^{YSZ}_{O_{2-}} - \frac{\Theta}{F}S^*_{Cu^+} \tag{10}$$

The kinetic hysteresis: subtracting Eq. (9) from Eq. (10) we obtain an equation for a kinetic thermopower hysteresis caused by the Soret effect:

$$\varepsilon^{(a)}_{t\to\infty} - \varepsilon^{(a)}_{t\to 0} = -t_{e^-}\cdot\frac{\Theta}{F}\cdot\frac{Q^*_{Cu}}{T} \cong -\frac{\Theta}{F}\cdot\frac{Q^*_{Cu}}{T} \tag{11}$$

The sign and the magnitude of Q^*_{Cu} decides on the orientation and the width of the hysteresis. Eq. (11) also shows that a material with a dominating ionic transference number ($t_{e^-} \cong 0$) will show a negligible hysteresis in an experiment employing ionic probes. Other cases are discussed in [35].

The fraction Θ of the total temperature difference being applied to the thermocell is included in the final result for the hysteresis, as the thermopower is a weighted average of the ionic thermopowers of YSZ and the sample. It can be omitted if the temperature difference for the evaluation of the thermopower is measured only along the sample.

2.2.2. The open thermocell

In this case the YSZ/cuprite interface is open to the gas atmosphere, i.e. the chemical potential of oxygen at the interface is controlled by the partial pressure of oxygen in the gas surrounding the cell and the local temperature.

$$\mathrm{Pt}'(a_{O_2})|\mathrm{YSZ}'|\mathrm{Cu}_{2-\delta}\mathrm{O}(a_{O_2})|\mathrm{YSZ}''\,|\mathrm{Pt}''(a_{O_2}) \xrightarrow[\nabla T]{} \tag{b}$$

Initial state ($t\to 0$, $\nabla\delta$=0): the thermopower in the initial state is independent from the boundary conditions for matter exchange, and so it identical for both cells and Eq. (41) also applies here, i.e. $\varepsilon^{(a)}_{t\to 0}=\varepsilon^{(b)}_{t\to 0}$.

The stationary state ($t\to\infty, j_{Cu}\neq 0$): in the stationary state the thermopower of cell (b) results as:

$$\varepsilon^{(b)}_{t\to\infty} = -\epsilon^{Pt}_{e^-} - \frac{1}{4F}S_{O_2} + \frac{\Theta}{2F}S_{Cu_2O} + (1-\Theta)\epsilon^{YSZ}_{O^{2-}} - \frac{\Theta}{F}\cdot\left[t_{Cu^+}\cdot S^*_{Cu^+} - t_{e^-}\left(-\frac{1}{2}S_{Cu_2O} + \frac{1}{4}S^\circ_{O_2} - \frac{1}{4}R\ln a_{O_2} + S^*_{e^-}\right)\right] \tag{12}$$

The kinetic hysteresis: subtracting Eq. (9) from Eq. (12) it results a different thermopower hysteresis:

$$\varepsilon^{(b)}_{t\to\infty} - \varepsilon^{(b)}_{t\to 0} = -t_{e^-}\frac{\Theta}{F}\cdot\left[\frac{1}{2}S_{Cu_2O} - \frac{1}{4}S^\circ_{O_2} + \frac{1}{4}R\ln a_{O_2} - \tilde{S}_{Cu}\right] \tag{13}$$

which can be simplified by assuming local equilibrium and $t_{e^-} \cong 1$:

$$\varepsilon^{(b)}_{t\to\infty} - \varepsilon^{(b)}_{t\to 0} = \frac{\Theta}{4F}\left(\underbrace{S^\circ_{O_2} - R\ln p_{O_2}}_{S_{O_2}(g)} - \tilde{S}_{O_2}\right) \tag{14}$$

This hysteresis offers information on the partial molar entropy of oxygen in the nonstoichiometric oxide but does not contain any information on the heat of transport.

3. Experimental

We constructed two different thermocells: (a) a closed cell of type I and (b) an open cell of type II. As starting materials we used copper metal rod (99.99% purity), single crystalline 10YSZ (99.99%, Fa. Kelpin, Kiel/Germany) and alumina ceramics (Haldenwanger, Berlin). We grew a cylindrical $Cu_{2-\delta}O$ polycrystal by one-dimensional growth from the elements within a thick-walled alumina tube of 15 mm length and 6 mm inner diameter. Before the growth experiment we drilled two small holes (0.5 mm) at a distance of 3 mm into the alumina tube with a laser and introduced two platinum wires (300 μm thickness) into the holes as electronic probes. One end of the alumina tube was closed with an alumina plate and some high temperature ceramic paste (Keramabond), then the copper rod (8 mm length, 5 mm thickness) was inserted.

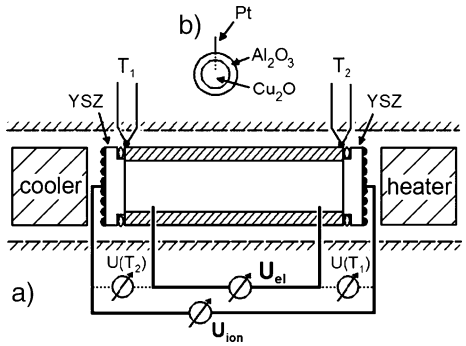

Fig. 2. (a) Galvanic cell for the measurement of the ionic thermopower of $Cu_{2-\delta}O$; (b) cross section of cell.

At a temperature of 1050 °C under nitrogen atmosphere (log a_{O_2}=−2.95) the copper rod had completely reacted within 8 weeks and had formed a compact and dense rod of copper(I)-oxide, which completely filled the alumina tube and also included the two platinum electrodes. After careful cooling the ends of the cuprite-filled alumina tube were capped and polished mechanically. Despite careful preparation the cuprite crystals and alumina tubes always showed some tiny microcracks due to the different thermal expansion coefficients. In order to seal these cracks in the alumina tube we covered them with some pieces of low-melting glass before the experiment.

3.1. The closed cell $Pt(O_2)|YSZ|Cu_{2-\delta}O|YSZ|Pt(O_2)$

Electrodes were cut as 2 mm thick plates from a cylindrical rod of 10YSZ single crystal (20 mm diameter). One side of each electrode was always polished carefully down to mirror-like finish with 6 μm diamond paste. By using an ultrasonic drill we cut a circular groove (1 mm deep) into the polished side and filled this groove with a 1.5 mm thick glass ring. During the later measurement this glass ring worked as a sealing of the electrode alumina interface. On the open back of each YSZ electrode we fixed a spherical piece of platinum mesh and a platinum lead wire with platinum paste. Two Pt/PtRh10 thermocouples were fixed to the cell at the interface between YSZ and alumina. The final cell is depicted schematically in Fig. 2.

The whole cell was placed in the alumina sample holder of a high temperature resistance furnace (SiC). The temperature gradient was established by a miniaturised heating element (Pt resistance heater) on one side of the cell and a cooling element (gas flow) on the other side. All experiments were performed under nitrogen atmosphere. The data were collected by a digital multimeter 2002 (Keithley Instruments) attached to a personal computer.

3.2. The open cell $Pt(O_2)|YSZ|Cu_{2-\delta}O|YSZ|Pt(O_2)$

The open cell is constructed almost identical to the closed cell. But here the interfaces between YSZ electrodes and cuprite are left open, i.e. no sealing glass but a thin stripe of platinum metal was introduced.

The combined heater/cooler was able to establish stable temperature differences of approx. 10 K within relatively short time, corresponding to gradients of approx. 20 K/cm. The actual temperature difference along the cell under transient conditions was not measured by the thermocouples, as this would have been not too erroneous. Rather we used the thermocouples only for the measurement of the mean temperature of the cell and for the measurement of the temperatures under stationary conditions. The temperature difference during the transient state was determined from the electronic thermovoltage of the cell $Pt/Cu_{2-\delta}O/Pt$, i.e. we used the sample itself together with the two platinum wires as a thermocouple. As cuprite has a negligible temperature dependence of its thermopower at the experimental conditions, this offers the opportunity to measure the temperature difference very precisely directly within the sample. For the evaluation of the temperature difference from the electronic thermopower data, we used the data given by Riess in [29].

4. Results

4.1. The closed cell

Before any thermopower experiment we tested the cell under isothermal conditions, measuring the ionic conductivity of cuprite under dc conditions at T=1030 °C. Under galvanostatic conditions we determined the stationary voltage drop across the cell. The results are depicted in Fig. 3.

As expected the cell resistance is non-ohmic due to polarisation effects at the YSZ/cuprite interface. From the slope at small polarisation currents we estimate a mean value for the ionic conductivity of $\sigma_{Cu^+}=9.6\cdot10^{-4}$ Ω/cm at $a_{O_2}=10^{-3}$ and T=1030 °C (cell constant l/A=2.12 cm^{-1}).

Fig. 4 shows typical raw data for the time series of the emf of both individual cells ($U(T_1)$ and $U(T_2)$) and of the

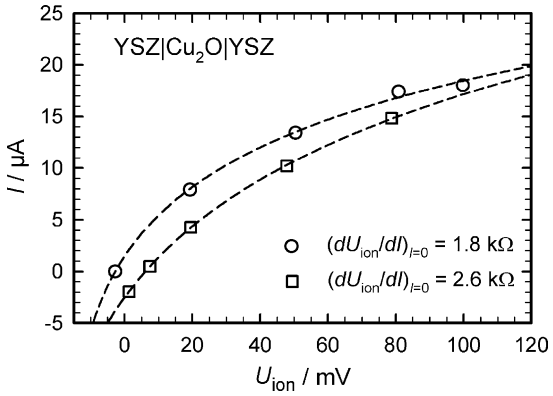

Fig. 3. Current/voltage measurement of the closed cell $Pt(O_2)|YSZ|Cu_{2-\delta}O|YSZ|Pt(O_2)$ at T=1030 °C and log a_{O_2}=−2.95. The two different symbols represent two independent measurements.

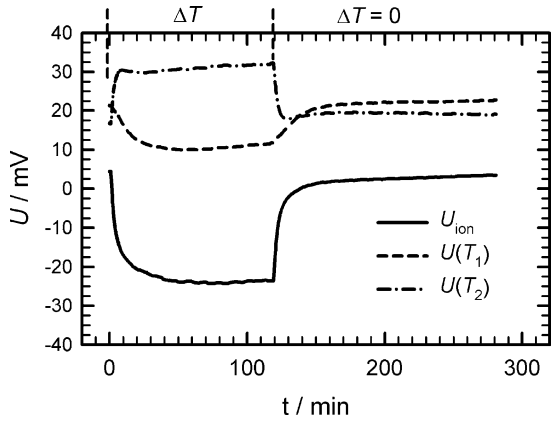

Fig. 4. Emf of both half cells $U(T_1)$ and $U(T_2)$ and thermovoltage of the thermocell I as a function of time during a typical thermopower experiment with the closed cell.

total cell emf (U_{ion}). Both half cells show a fast emf change in the beginning, simultaneously with the temperature change, and a slow change after the establishment of the stationary temperature profile. This slow change indicates the kinetic demixing due to the Soret effect. The measurements always showed this typical behavior. At the beginning of the experiments we mostly observed a constant voltage off-set of a few mV which we attribute to a slight temperature gradient even before the experiment.

A plot of the ionic thermovoltage $U_{ion}(\Delta T)$ versus the electronic thermovoltage $U_{el}(\Delta T)$ for a typical experiment is depicted in Fig. 5.

The hysteresis shows the expected form (cf. [35]). The average temperature of the cell was increased by 30 K during the experiment, and thus, the curve is not perfectly symmetric. We performed several experiments of this kind at the same oxygen activity of $\log a_{O_2}=-2.95$ and within the temperature range from 1200 K to 1260 K, see the results in Fig. 6. The data points representing much smaller results

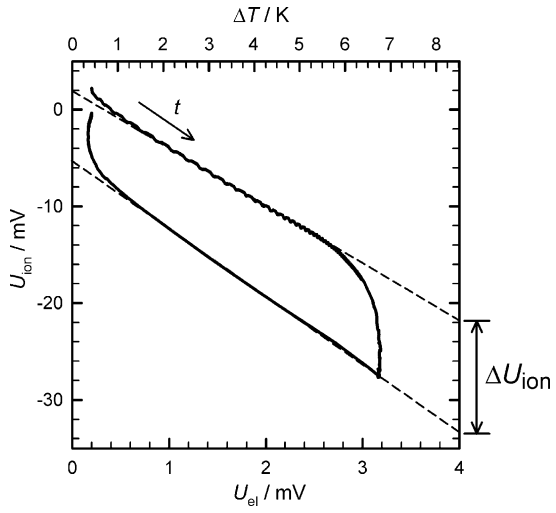

Fig. 5. Ionic thermopower U_{ion} versus electronic thermopower U_{el} of $Cu_{2-\delta}O$ at a mean temperature of T=985 °C, $\log a_{O_2}=-2.95$ and $\Delta T/\Delta x$=20 K/cm; closed cell.

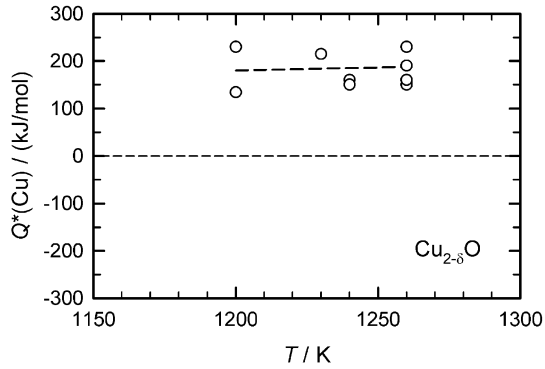

Fig. 6. Data for the heat of transport of copper metal obtained from various experiments with cell I (closed cell).

correspond to two experiments during which the cooler/heater system was not working properly, and we excluded these from the averaging. The average value for the heat of transport is determined as

$$Q^*_{Cu} \approx (180 \pm 80)\ \mathrm{kJ/mol},$$

corresponding to an average value for the thermopower hysteresis of $\varepsilon^{(a)}_{t\to\infty} - \varepsilon^{(a)}_{t\to 0} = -1.47$ mV/K.

Compared to the closed cell the open cell always showed a very small hysteresis of up to 2 mV for temperature differences of up to 11 K. Thus, the hysteresis of cell II is $\varepsilon^{(b)}_{t\to\infty} - \varepsilon^{(b)}_{t\to 0} = 1.18$ mV/K.

5. Discussion

5.1. Point defect structure of $Cu_{2-\delta}O$

Cuprite crystallizes in a cubic structure with a bcc oxygen sublattice. The copper ions form tetrahedra around some of the oxygen ions. At T=1000 °C, cuprite is stable only within the oxygen activity range of $-6<\log(a_{O_2})<-1$ [25]. A number of experimental determinations of the deviation from stoichiometry have been published which differ considerably in their results. The most recent data by Porat and Riess correspond to $-1.8\cdot 10^{-3}<\delta<4.5\cdot 10^{-3}$ at T=1245 K [26], i.e. both metal excess and deficit can be adjusted in cuprite. Wagner was the first to propose a defect structure for the metal deficient region based exclusively on the existence of cation vacancies and electron holes [27]. Xue and Dieckmann proposed a model which covers the complete range of homogeneity by assuming the existence of (neutral) cation vacancies at high oxygen activities and (neutral) oxygen vacancies at low oxygen activities as majority defects [25]. Porat and Riess include copper interstitials at low temperatures and low oxygen activities in their model [26]. Despite some discrepancies, there is no doubt that cation vacancies are the majority defects at high oxygen activities, and that their average charge number seems to be smaller than −1.

Formulating the oxidation of cuprite by the formation of neutral vacancies:

$$\frac{1}{2}O_{2(g)} = O_O^{\times} + 2V_{Cu}^{\times} \quad K(T = 1273\ \mathrm{K}) = 7 \cdot 10^{-3} \qquad (15)$$

and accounting for the formation of charged vacancies by the dissociation equilibrium,

$$2V_{Cu}^{\times} = 2V_{Cu}^{'} + 2h^{\bullet} \qquad (16)$$

Porat and Riess determine the formation enthalpy and entropy of neutral vacancies as $\Delta_f H_V^{\circ}$=60.2 kJ/mol and $\Delta_f S_V^{\circ}$=5.5 J/K mol at T=1200 K which corresponds to a site fraction of neutral copper vacancies $x_V \approx 10^{-3}$ at a_{O_2}=10^{-3}. Cuprite is a p-semiconductor with a small ionic transference number and an electronic conductivity which depends strongly on the oxygen activity [27,29]. The electronic majority defects are electron holes at high oxygen activity, being formed by the dissociation of the neutral vacancies. At low temperatures electrons influence the electronic transport properties but a complete transition from p- to n-conduction is not observed [29]. The optical band gap at T=1200 K equals ΔE_g=1.4 eV [38].

Summarizing the knowledge on the defect properties, we can safely assume that any diffusion at high oxygen activities and high temperature is based on cation vacancy motion. The charge state of the vacancies is not known exactly. In terms of defects with discrete charges we have to assume that both singly negatively charged and neutral vacancies are present.

5.2. Ionic transport in $Cu_{2-\delta}O$

The diffusion coefficient of the copper cations is higher by more than two orders of magnitude than the mobility of the oxygen anions [31,32,40]. Therefore we can assume that oxygen anions are virtually immobile and do not contribute to the ionic transference and the thermodiffusion. The chemical diffusion coefficient $\tilde{D}_{Cu}$ of copper has been determined to be within the orders of 10^{-4} cm^2/s–10^{-5} cm^2/s between T=1000 K and T=1250 K [30].

To our knowledge, data for the ionic conductivity have only been measured at a relatively low temperature of T=400 °C by employing CuBr/Cu electrodes [39]. At 1000 °C, Gundermann and Wagner determined the ionic transference number $t_{Cu^+} \approx 5 \cdot 10^{-4}$ [41]. Taking the much higher electronic conductivity σ_{e^-}=5.25 S/cm [29] as the total conductivity, the ionic conductivity results as σ_{Cu^+}=$2.6 \cdot 10^{-3}$ S/cm. This value is larger by a factor of 2.5 than our experimental value, but fits well by the order of magnitude.

Petersen and Wiley [31] measured the copper tracer diffusion coefficient which can also be used to evaluate the ionic conductivity by the Nernst–Einstein relation:

$$\sigma_{Cu^+} = (zF)^2 \frac{c_{Cu} D_{Cu}}{RT} \qquad (17)$$

D_{Cu} denotes the self-diffusion coefficient which is related to the tracer diffusions coefficient D_{Cu}^* by the relation D_{Cu}=D_{Cu}^* /f with the geometrical correlation factor f=0.74 [31]. $c_{Cu} \approx 0.084$ mol/cm^3 represents the molar concentration of copper in the oxide which can be evaluated from the molar volume (c_{Cu}=2/V_m) [36]. For T=1030 °C and log $a_{O_2} \approx -3$ Peterson reports the value $D_{Cu} \approx 2.7 \cdot 10^{-8}$ cm^2/s [31]. The value resulting for the ionic conductivity σ_{Cu^+}=$2.6 \cdot 10^{-3}$ S/cm from Eq. (17) is also larger by a factor of 2.6 than our experimental value, but fits very well with Gundermann's and Wagner's ionic transference result. We assume that our experimental result is influenced by polarisation effects at the interfaces between YSZ and the oxide, as we only performed a two-electrode measurement.

Peterson and Wiley report a value of ΔH_m=92 kJ/mol for the migration enthalpy (activation energy) of copper [31], not distinguishing between charged and neutral copper vacancies. It should be noted that the correlation coefficient for copper diffusion via vacancies in the cuprite lattice, which has been determined experimentally by Peterson and Wiley, has yet not been confirmed by a theoretical calculation.

5.3. Stationary demixing in the Soret state

Combining Eqs. (5) and (6), we obtain the flux equation for the copper metal. In the stationary state of the closed cell (a) any mass flux equals zero:

$$j_{Cu} = -L_{Cu}\left[\nabla \mu_{Cu} + \left(\tilde{S}_{Cu} + \frac{Q_{Cu}^*}{T}\right)\nabla T\right] \equiv 0 \qquad (18)$$

Using the Gibbs–Duhem relation $2\nabla\mu_{Cu} + \nabla\mu_O = \nabla\mu_{Cu_2O} \rightharpoonup 0$ and the differential $d\mu_O = (\frac{\partial \mu_O}{\partial \delta})_T d\delta + (\frac{\partial \mu_O}{\partial T})_\delta dT$ for the chemical potential of oxygen, the following equation results:

$$\nabla\delta = \frac{4}{\left(\frac{\partial \ln a_{O_2}}{\partial \delta}\right)_T} \frac{Q_{Cu}^*}{RT} \frac{\nabla T}{T} \qquad (19)$$

Inserting the data for the thermodynamic factor $(\partial \ln a_{O_2}/\partial\delta)_{1260\ \mathrm{K}}$=$7.9 \cdot 10^3$ at log a_{O_2}=−2.95 from the literature [25,37] and assuming Q_{Cu}^*=180 kJ/mol, we calculate a Soret effect of:

$$\frac{d\delta}{dT} = 6.9 \cdot 10^{-6}\ \mathrm{K}^{-1} \qquad (20)$$

The deviation from stoichiometry at T=1260 K and log a_{O_2}=−2.95 approximates to $\delta \approx 4 \cdot 10^{-4}$. Thus, the relative Soret effect equals 1.7%/K. With a typical temperature difference of 6.5 K during our experiments this leads to a concentration gradient of copper which corresponds to 19% of the full phase width of $Cu_{2-\delta}O$. The stationary demixing effect under Soret conditions, i.e. in the case of a closed system, is considerably large and may even lead to a decomposition of the material.

5.4. Stationary demixing of the open system

If the crystal is open to the gas atmosphere (cell(b)), the Soret state is not attained, and the crystal will be reduced on one side and oxidised on the other side. In effect, the crystal will slowly move along the temperature gradient, and a quasi-stationary state can be assumed for the concentration gradient within the moving system, see Fig. 7. This is well known for the case of an isothermal chemical potential gradient [7]. Assuming local equilibrium with the gas phase and again using the Gibbs–Duhem relation, we find for the open case:

$$\nabla\delta = \frac{\bar{S}_{O_2} - S_{O_2}(O_2)}{R\left(\frac{\partial \ln a_{O_2}}{\partial \delta}\right)_T} \frac{\nabla T}{T} \tag{21}$$

The composition gradient within the open system is only determined by the thermodynamics of the oxide and the gas phase, i.e. the heat of transport cannot be obtained from a thermodiffusion experiment with open surfaces. If the local equilibrium at the surface is not established due to a slow surface kinetics, then the kinetic control by the heat of transport (Soret effect) will superpose to the thermodynamic control by the gas phase. If the rate of the surface reaction tends to zero, then the local equilibrium between oxide and molecular oxygen in the gas phase is completely lost, and the Soret state (see above) is obtained.

With Eq. (14) we can calculate the thermopower hysteresis of an open thermocell from entropy data for oxygen in the gas phase and the oxide. Using $S^{\circ}_{O_2}(O_2)$=252 J/K mol [37] within the temperature range between T=1000 °C and 1025 °C, and $\bar{S}_{O_2}(Cu_{2-\delta}O)$=162 J/K mol within the same temperature range [25] for an oxygen activity of log a_{O_2}=−2.95 we find that:

$$\varepsilon_{II}^{t\to\infty} - \varepsilon_{II}^{t\to 0} = 0.38\ \text{mV/K} \tag{22}$$

For a typical experimental temperature difference of ΔT= 11 K the hysteresis results as 4.18 mV. Using the same data, we calculate for the stationary demixing by using Eq. (21):

$$\frac{d\delta}{dT} = -1.09\cdot 10^{-6}\ \text{K}^{-1} \tag{23}$$

The relative demixing corresponds to $1/\delta \cdot d\delta/dT$= −0.3%/K, i.e. it shows the opposite direction to the demixing in the Soret experiment and is smaller by almost one order of magnitude.

It has to be noted that the results base on the subtraction of two large numbers in the numerator of Eqs. (22) and (21), and thus, the error is relatively large. Our experiment gives a result of 2 mV for the thermovoltage hysteresis under open conditions. This is the half of the theoretical value. In view of both the uncertainty in the theoretical estimation and the experimental error, the agreement is satisfactorily.

5.5. The heat of transport of the copper vacancy

The heat of transport of the copper metal is the sum of the independent heats of transport $Q^*_{Cu^+}$ and $Q^*_{e^-}$ of the building units copper ions and electrons:

$$Q^*_{Cu} = Q^*_{Cu} + Q^*_{e^-} \tag{24}$$

These heats of transport are related to the heats of transport of the mobile point defects (structure elements), see Janek and Korte [34] for a detailed analysis of different heats of transport. The heats of transport of delocalised electronic charge carriers are usually in the order of RT, which corresponds to approx. 10 kJ/mol at T=1000 K in the present case. This is much smaller than the measured heat of transport, and therefore we neglect it in the following analysis. Thus, the measured heat of transport Q^*_{Cu} can be approximated by the heat of transport $Q^*_{Cu^+}$ of the cations. And as the cations migrate predominantly by vacancies, the heat of transport of the ions can be identified with the negative heat of transport of the copper vacancies (see [34] for general relations):

$$-Q^*_V = Q^*_{Cu^+} \simeq Q^*_{Cu} \approx 180\ \text{kJ/mol} \tag{25}$$

5.6. Comparison with theory

The theoretical understanding of the Soret effect in condensed phases is still incomplete to date. Serious achievements have been made quite recently by molecular dynamic simulations of simple solids (noble gas crystals, gold) by Jones et al. [42–44]. Based on a formalism by Gillan [45], Jones et al. determine the heat of transport of atoms in noble gas crystals moving by a simple vacancy

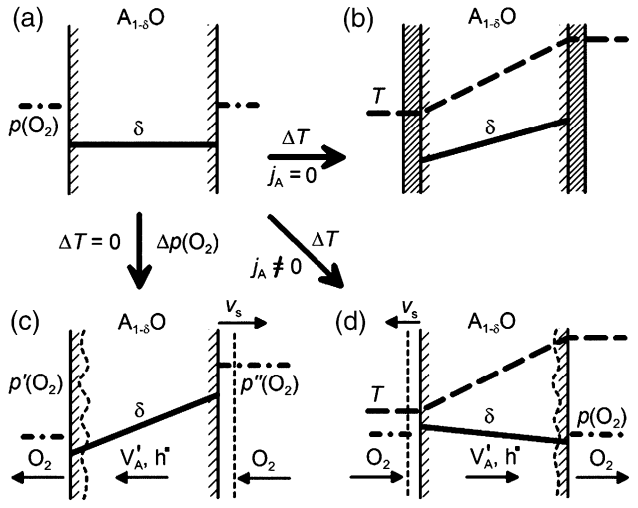

Fig. 7. A nonstoichiometric binary oxide under different experimental conditions: (a) equilibrium, (b) Soret effect, (c) chemical potential gradient, (d) thermodiffusion.

mechanism. Contradictory to older models for the heat of transport (e.g. Wirtz [46], Brinkman [47], LeClaire [48] and Schottky [49]), they obtain heats of transport being larger than the migration enthalpy of the atomic jumps. Always they obtain positive heats of transport for atoms moving by a vacancy mechanism, and they formulate the relation

$$\frac{Q^*_V(\exp)}{\Delta H_{m,V}(\exp)} \approx -2 \tag{26}$$

A comparison of the experimental heat of transport of the vacancies $Q^*_V = -180$ kJ/mol with the migration enthalpy of copper ions $\Delta H_{m,Cu} = 92$ kJ/mol results in:

$$Q^*_V \approx -2 \cdot \Delta H_{m,Cu} \tag{27}$$

and agrees well with their theoretical finding.

5.7. Comparison with other systems

The knowledge on thermodiffusion in non-metal systems is limited and it is poor for oxide systems. One of the main reasons is that the experimental determination of heats of transport is difficult, as already discussed above. Only the heats of transport of neutral components can be determined experimentally. To derive information on the heat of transport of individual point defects, we have to analyse the component heat of transport on the basis of the defect structure and kinetics of the material. In metals or metal-like semiconductors, the electron wind complicates the evaluation of the pure phonon contribution to the heat of transport. In addition, the experiment itself suffers from the problem of realizing sufficiently high temperature gradients and of fixing the frame of reference. Ionic compounds with at least one immobile sublattice provide much less experimental difficulties. The immobile sublattice provides a natural frame of reference, and electrochemical cells offer favourable means for measuring local chemical activities. Doing so, a number of mixed-conducting binary compounds have been studied so far [13,15–20,50–59], but only a few quantitative results for Q^* have been evaluated.

Experiments on nonstoichiometric silver chalcogenides probably provide the most precise data for the heat of transport of a mobile component (silver metal) to date. However, the evaluation of heats of transport of individual defects is complicated by the fact that the heat of transport of the neutral metal is the sum of the independent heats of transport ions and electrons. Even neglecting the electronic contribution, the interpretation of the remaining ionic heat of transport is complicated since it is composed of contributions of all mobile defects [19,55–59].

A summary of available data on heats of transport of defects and their migration enthalpies is given in Table 1.

Table 1
Heats of transport of point defects or components in nonstoichiometric compounds

Material	Q^* (kJ/mol)	ΔH_m (kJ/mol)	References
$Cu_{2-\delta}O$	$-180^{(*)}$	92	this work
$UO_{2\pm\delta}$	0 to 100	53	[19,60]
$CeO_{2-\delta}$	23 to 100	17 to 96	[16,61]
ZrO_2(+8m/oY_2O_3)	90	106	[17,62]
β-$Ag_{2+\delta}S$	−2 to 7, 5	6, 3	[57]
α-$Ag_{2+\delta}S$	−38 to 45	6, 3	[58]
α-$Ag_{2+\delta}Se$	−20 to 38	15, 5	[55]
AgCl	−65	30	[35,63]

(*) Value for the heat of transport of the majority atomic defect. In all other cases the analysis in terms of individual defects is ambiguous.

The comparison of the heats of transport with migration enthalpy in Table 1 suffers from several problems. Firstly, the analysis of the thermodiffusion or Soret effect in terms of individual point defects relies on the knowledge of the defect structure and the majority types of defects. These are not always known with sufficient precision. Secondly, both heats of transport and migration enthalpies have usually been determined by different authors on different samples at different conditions. Thus, Table 1 necessarily gives only a very rough idea about the experimental relation been the heat of transport and the migration enthalpy. In fact, the current experimental knowledge is still poor, and more studies on well defined model systems with well understood defect structure and kinetics are required for a better understanding.

6. Conclusions

The stationary composition gradient within a nonstoichiometric oxide in a temperature gradient depends on the boundary conditions at the surfaces of the material. The Soret effect alone is only observed if the surfaces are completely closed for matter exchange between the oxide and the gas phase. In this case, a stationary gradient of the nonstoichiometry is established which is determined by the heat of transport as a kinetic quantity. For $Cu_{2-\delta}O$ we find a Soret effect of 1.7%/K at our experimental conditions. If the surfaces are open for matter exchange with the gas atmosphere, the chemical potential of the gas controls the composition of the oxide at both the hot and the cold end. The gradient of the nonstoichiometry is in this case not kinetically controlled by the heat of transport, rather it is exclusively determined by the thermodynamics of the system. In the case of an open $Cu_{2-\delta}O$ sample, the gradient is counter-directed and smaller by one order of magnitude than in the Soret experiment.

The experiments and the theoretical analysis show that the evaluation of the heat of transport from the Soret effect requires a careful design of the non-isothermal experiment. Only if the sample is completely encapsulated and isolated from the gas phase, the Soret effect can be observed.

Glossary

a_k thermodynamic activity of the component (species) k

c_k molar concentration of the component (species) k in mol/m^3

c_p molar heat capacity in J/K mol

$\tilde{D}_\mathrm{k}$ chemical diffusion coefficient of the mobile component$k$ in m^2/s

D_k^T thermodiffusion coefficient of the mobile component k in m^2/s

D_k self-diffusion coefficient of the mobile component k in m^2/s

F Faraday's constant, 96,484.8 C/mol

j_k (one-dimensional) molar flux of the component (species) k in mol/m^2 s

L_k phenomenological transport coefficient of the mobile component k

Q_k^* reduced heat of transport of the mobile component (species) k in J/mol

R gas constant, 8.31441 J/K mol

$\bar{\mathrm{S}}_k$ partial molar entropy of the component (species) k in a compound with variable composition in J/K mol

S_k molar entropy of the compound/element k in J/K mol

S_k° molar standard entropy of the compound/element k in J/K mol

S_k^* entropy of transport of the mobile component (species) k in J/K mol

t_k electric transference number of mobile component (species) k

T absolute temperature in K

$U(T)$ emf of a galvanic cell as a function of temperature in V

$U_\mathrm{ion}(\Delta T)$ ionic thermovoltage (thermo emf) of the thermogalvanic cell in V as a function of the temperature difference

$U_\mathrm{el}(\Delta T)$ electronic thermovoltage (thermo emf) of the thermogalvanic cell in V as a function of the temperature difference

V_m molar volume of $\mathrm{A}_\nu\mathrm{X}$ in m^3/mol

v_k velocity of the mobile component k in m/s

z_k charge number of the mobile charge carrier k

δ deviation from stoichiometry

ε thermopower of a thermogalvanic cell (general case) in V/K

$\varepsilon_{t\to 0}^{(\mathrm{a})}$ thermopower of a closed thermogalvanic cell in the initial state in V/K

$\varepsilon_{t\to \infty}^{(\mathrm{a})}$ thermopower of a closed thermogalvanic cell in the Soret state in V/K

$\varepsilon_{t\to 0}^{(\mathrm{b})}$ thermopower of an open thermogalvanic cell in the initial state in V/K

$\varepsilon_{t\to \infty}^{(\mathrm{b})}$ thermopower of an open thermogalvanic cell in the Soret state in V/K

ϵ_k^C absolute thermopower of the compound C (charge carrier k) in V/K

μ_k chemical potential of the component (species) k in J/mol

λ thermal conductivity in J/Kms

$\tilde{\mu}_\mathrm{k}$ electrochemical potential of the component (species) k in J/mol

ϕ electric potential in V

σ_k electrical conductivity of charge carrier k in $(\Omega\ \mathrm{cm})^{-1}$

Θ fraction of total temperature difference along the thermogalvanic cell which is applied to the mixed conductor

Acknowledgement

This project was funded by the DFG within the SFB 173 at the University of Hannover and a subsequent DFG project. Financial support of the FCI (Fonds der Chemischen Industrie) is also gratefully acknowledged. We thank A. B. Lidiard (Reading, UK) for his continuous and stimulating support, and we thank H. I. Yoo (Seoul, Korea) for helpful comments. Without his perseverance this study would not have been performed. This paper was finalised during an extended stay of JJ at Tohoku University (Sendai/Japan) as visiting professor. He expresses his gratitude to Prof. Mizusaki and Prof. Kawada for their hospitality and support.

Appendix A

For both thermocells I and II the thermovoltage U is defined as the difference in the Galvani potential ϕ of the two platinum ends (being kept at the same temperature):

$$U = \Delta\phi = \phi(\mathrm{Pt}'', T) - \phi(\mathrm{Pt}', T)$$
$$= -\frac{1}{F}[\tilde{\mu}_{\mathrm{e}^-}(\mathrm{Pt}'', T) - \tilde{\mu}_{\mathrm{e}^-}(\mathrm{Pt}', T)] \quad (28)$$

Here $\tilde{\mu}_{\mathrm{e}^-}$ denotes the electrochemical potential of electrons (Fermi level). Introducing the temperature difference along the platinum connectors,

$$\Delta\tilde{\mu}_{\mathrm{e}^-}(\mathrm{Pt}, T) = \tilde{\mu}_{\mathrm{e}^-}(\mathrm{Pt}'', T) - \tilde{\mu}_{\mathrm{e}^-}(\mathrm{Pt}', T)$$
$$= [\tilde{\mu}_{\mathrm{e}^-}(\mathrm{Pt}'', T) - \tilde{\mu}_{\mathrm{e}^-}(\mathrm{Pt}'', T + \Delta T)]$$
$$+ \tilde{\mu}_{\mathrm{e}^-}(\mathrm{Pt}'', T + \Delta T) - \tilde{\mu}_{\mathrm{e}^-}(\mathrm{Pt}', T)$$
$$= -\Delta\tilde{\mu}_{\mathrm{e}^-}(\mathrm{Pt}, \Delta T) + \tilde{\mu}_{\mathrm{e}^-}(\mathrm{Pt}'', T + \Delta T)$$
$$- \tilde{\mu}_{\mathrm{e}^-}(\mathrm{Pt}', T) \quad (29)$$

and assuming local equilibrium at both surfaces $\mathrm{Pt}(\mathrm{O}_2)|$YSZ

$$\mu_{\mathrm{O}_2}(\mathrm{g}) = 2\tilde{\mu}_{\mathrm{O}^{2-}}(\mathrm{YSZ}) - 4\tilde{\mu}_{\mathrm{e}^-}(\mathrm{Pt}) \quad (30)$$

we obtain the following relation:

$$\begin{aligned}\Delta\tilde{\mu}_{e^-}(\mathrm{Pt},T) = & -\Delta\tilde{\mu}_{e^-}(\mathrm{Pt},\Delta T)\\ & -\frac{1}{4}\left[\mu''_{O_2}(g,T+\Delta T)-\mu'_{O_2}(g,T)\right]\\ & +\frac{1}{2}\tilde{\mu}_{O^{2-}}(YSZ'',T+\Delta T)\\ & -\frac{1}{2}\tilde{\mu}_{O^{2-}}(YSZ',T). \end{aligned} \tag{31}$$

Here $\tilde{\mu}_{O^{2-}}$ denotes the electrochemical potential of oxygen anions in YSZ. Introducing the parameter Θ (see Eq. (8)) it follows

$$\begin{aligned}\Delta\tilde{\mu}_{e^-} = & \Delta\tilde{\mu}_{e^-}(\mathrm{Pt},\Delta T)-\frac{1}{4}\Delta\mu_{O_2}(g,\Delta T)\\ & +\frac{1}{2}\left\{\left[\tilde{\mu}_{O^{2-}}(YSZ'',T+\Delta T)\right.\right.\\ & \left.-\tilde{\mu}_{O^{2-}}\left(YSZ'',T+\frac{1}{2}(1+\Theta)\Delta T\right)\right]\\ & \left.+\tilde{\mu}_{O^{2-}}\left(YSZ'',T+\frac{1}{2}(1+\Theta)\Delta T\right)\right\}\\ & -\frac{1}{2}\left\{\left[\tilde{\mu}_{O^{2-}}-(YSZ',T)\right.\right.\\ & \left.-\tilde{\mu}_{O_{2-}}\left(YSZ',T+\frac{1}{2}(1-\Theta)\Delta T\right)\right]\\ & \left.+\tilde{\mu}_{O_{2-}}\left(YSZ',T+\frac{1}{2}(1-\Theta)\Delta T\right)\right\}\\ = & -\Delta\tilde{\mu}_{e^-}(\mathrm{Pt},\Delta T)-\frac{1}{4}\Delta\mu_{O_2}(\Delta T)\\ & +\frac{1}{2}\Delta\tilde{\mu}_{O_{2-}}\left(YSZ'',\frac{1}{2}(1-\Theta)\Delta T\right)\\ & +\frac{1}{2}\Delta\tilde{\mu}_{O_{2-}}\left(YSZ',\frac{1}{2}(1-\Theta)\Delta T\right)\\ & +\frac{1}{2}\tilde{\mu}_{O_{2-}}\left(YSZ'',T+\frac{1}{2}(1+\Theta)\Delta T\right)\\ & -\frac{1}{2}\tilde{\mu}_{O_{2-}}\left(YSZ',T+\frac{1}{2}(1-\Theta)\Delta T\right). \end{aligned} \tag{32}$$

Also assuming local equilibrium for the exchange of oxygen ions at the interfaces YSZ/$Cu_{2-\delta}O$,

$$\tilde{\mu}_{O^{2-}}(YSZ)=\tilde{\mu}_{O^{2-}}(Cu_{2-\delta}O) \tag{33}$$

and using the formation equilibrium:

$$\tilde{\mu}_{O^{2-}}=\mu_{Cu_2O}-2\tilde{\mu}_{Cu^+} \tag{34}$$

it follows from Eqs. (32)–(34):

$$\begin{aligned}\Delta\tilde{\mu}_{e^-} = & -\Delta\tilde{\mu}_{e^-}(\mathrm{Pt},\Delta T)-\frac{1}{4}\Delta\mu_{O_2}(\Delta T)\\ & +\Delta\tilde{\mu}_{O^{2-}}\left(YSZ,\frac{1}{2}(1-\Theta)\Delta T\right)\\ & +\frac{1}{2}\mu_{Cu_2O}\left(T+\frac{1}{2}(1+\Theta)\Delta T\right)\\ & -\tilde{\mu}_{Cu^+}\left(T+\frac{1}{2}(1+\Theta)\Delta T\right)\\ & -\frac{1}{2}\mu_{Cu_2O}\left(T+\frac{1}{2}(1-\Theta)\Delta T\right)\\ & +\tilde{\mu}_{Cu^+}\left(T+\frac{1}{2}(1-\Theta)\Delta T\right)\\ = & -\tilde{\mu}_{e^-}(\mathrm{Pt},\Delta T)-\frac{1}{4}\mu_{O_2}(\Delta T)\\ & +\Delta\tilde{\mu}_{O^{2-}}\left(YSZ,\frac{1}{2}(1-\Theta)\Delta T\right)\\ & +\frac{1}{2}\Delta\mu_{Cu_2O}(\Theta\cdot\Delta T)-\Delta\tilde{\mu}_{Cu^+}(\Theta\cdot\Delta T) \end{aligned} \tag{35}$$

We assume that the Seebeck coefficient of YSZ is constant within a temperature interval of 15 K. This is confirmed by measurements of Yoo and Hwang [17]. Taking Eq. (28) into account, dividing by dT and using the definition of the absolute thermopower,

$$\epsilon_k \equiv \frac{1}{z_kF}\left(\frac{\mathrm{d}\tilde{\mu}_k}{\mathrm{d}T}\right) \tag{36}$$

we end up with Eq. (7):

$$\begin{aligned}\varepsilon \equiv \frac{\mathrm{d}\phi}{\mathrm{d}T} = & \frac{1}{F}\frac{\mathrm{d}\tilde{\mu}_{e^-}(\mathrm{Pt})}{\mathrm{d}T}+\frac{1}{4F}\frac{\mathrm{d}\mu_{O_2}}{\mathrm{d}T}-\frac{(1-\Theta)}{2F}\\ & \times\frac{\mathrm{d}\tilde{\mu}_{O^{2-}}(YSZ)}{\mathrm{d}T}-\frac{\Theta}{2F}\frac{\mathrm{d}\mu_{Cu_2O}}{\mathrm{d}T}+\frac{\Theta}{F}\frac{\mathrm{d}\tilde{\mu}_{Cu^+}}{\mathrm{d}T}\\ = & -\epsilon^{Pt}_{e^-}-\frac{1}{4F}S_{O_2}+\frac{1}{2F}\Theta\cdot S_{Cu_2O}+(1-\Theta)\epsilon^{YSZ}_{O^{2-}}\\ & +\Theta\cdot\epsilon^{Cu_2O}_{Cu^+} \end{aligned} \tag{37}$$

A.1. The closed thermocell

Initial state ($t\to 0$, $\nabla\delta=0$): in the very beginning of a thermodiffusion experiment we observe the coupled fluxes of ions and electrons, $\vec{j}_{Cu^+}=\vec{j}_{e^-}$, leading from Eqs. (5) and (6) to

$$-L_{Cu^+}\left[\frac{\mathrm{d}\tilde{\mu}_{Cu^+}}{\mathrm{d}x}+S^*_{Cu^+}\frac{\mathrm{d}T}{\mathrm{d}x}\right]=-L_{e^-}\left[\frac{\mathrm{d}\tilde{\mu}_{e^-}}{\mathrm{d}x}+S^*_{e^-}\frac{\mathrm{d}T}{\mathrm{d}x}\right] \tag{38}$$

Inserting

$$\frac{\mathrm{d}\tilde{\mu}_{\mathrm{Cu}^+}}{\mathrm{d}x} = \frac{\mathrm{d}\tilde{\mu}_{\mathrm{Cu}^+}}{\mathrm{d}T}\,\frac{\mathrm{d}T}{\mathrm{d}x} \tag{39}$$

and assuming local equilibrium ($Cu^+ + e^- = Cu$),

$$\frac{\mathrm{d}\tilde{\mu}_{\mathrm{e}^-}}{\mathrm{d}x} = \frac{\mathrm{d}\tilde{\mu}_{\mathrm{e}^-}}{\mathrm{d}T}\,\frac{\mathrm{d}T}{\mathrm{d}x} = \left(\frac{\mathrm{d}\mu_{\mathrm{Cu}}}{\mathrm{d}T} - \frac{\mathrm{d}\tilde{\mu}_{\mathrm{Cu}^+}}{\mathrm{d}T}\right)\frac{\mathrm{d}T}{\mathrm{d}x} \tag{40}$$

we obtain the electrochemical potential gradient of the copper ions, i.e. the ionic thermopower of the oxide, by inserting Eqs. (39) and (40) in Eq. (38):

$$\left(\epsilon^{\mathrm{Cu_2O}}_{\mathrm{Cu}^+}\right)_{t\to 0} = \frac{1}{F}\left(\frac{\mathrm{d}\tilde{\mu}_{\mathrm{Cu}^+}}{\mathrm{d}T}\right)_{t\to 0}$$

$$= \frac{1}{F}\left[t_{\mathrm{e}^-}(S^*_{\mathrm{e}^-} - \bar{S}_{\mathrm{Cu}}) - t_{\mathrm{Cu}^+}S^*_{\mathrm{Cu}^+}\right] \tag{41}$$

The transference numbers t_i of the charge carriers ($t_{\mathrm{e}^-} \equiv L_{\mathrm{e}^-}/(L_{\mathrm{Cu}^+}+L_{\mathrm{e}^-})$ and $t_{\mathrm{Cu}^+}=1-t_{\mathrm{e}^-}\equiv L_{\mathrm{Cu}^+}/(L_{\mathrm{e}^-}+L_{\mathrm{Cu}^+})$) determine the contributions of the transported entropies S^*_i of the charge carriers to the ionic thermopower, together with the partial molar entropy $\bar{S}_{\mathrm{Cu}}$ of copper in the compound. Inserting Eq. (41) into Eq. (7) we obtain Eq. (9).

The Soret state ($t\to\infty$, $j_{\mathrm{Cu}}=0$): under stationary conditions we find that $\vec{j}_{\mathrm{Cu}^+} = \vec{j}_{\mathrm{e}^-} = 0$ and the composition gradient is maximal. With Eq. (5) we formulate

$$j_{\mathrm{Cu}^+} = -L_{\mathrm{Cu}^+}\left[\frac{\mathrm{d}\tilde{\mu}_{\mathrm{Cu}^+}}{\mathrm{d}x} + \left(\bar{S}_{\mathrm{Cu}^+} + \frac{Q^*_{\mathrm{Cu}^+}}{T}\right)\frac{\mathrm{d}T}{\mathrm{d}x}\right] = 0 \tag{42}$$

and after rearranging we obtain:

$$\left(\epsilon^{\mathrm{Cu_2O}}_{\mathrm{Cu}^+}\right)_{t\to\infty} = \frac{1}{F}\left(\frac{\mathrm{d}\tilde{\mu}_{\mathrm{Cu}^+}}{\mathrm{d}T}\right)_{\substack{t\to\infty \\ j=0}} = -\frac{1}{F}S^*_{\mathrm{Cu}^+} \tag{43}$$

The ionic thermopower in the stationary state is determined by the transported entropy of the ions. Inserting Eq. (43) into Eq. (7) we obtain Eq. (10).

A.2. The open thermocell

If the surfaces of the oxide sample are open for oxygen access from the gas phase, chemical diffusion is superposed to thermodiffusion. The initial state is identical to the case of the closed cell.

The stationary state ($t\to\infty$, $j_{\mathrm{Cu}}\neq 0$): we begin the analysis again with coupled fluxes of ions and electrons, $\vec{j}_{\mathrm{Cu}^+} = \vec{j}_{\mathrm{e}^-}$. The chemical potentials at the ends of the crystal are now controlled by the gas phase activity of oxygen. Assuming local equilibrium at the ends of the crystal,

$$\frac{1}{2}\mathrm{O_2} + 2\mathrm{Cu} = \mathrm{Cu_2O} \tag{44}$$

the chemical potential of copper metal equals

$$\mu_{\mathrm{Cu}} = \frac{1}{2}\mu_{\mathrm{Cu_2O}} - \frac{1}{4}\mu^\circ_{\mathrm{O_2}} - \frac{1}{4}RT\ln a_{\mathrm{O_2}} \tag{45}$$

and for the temperature differential we find:

$$\frac{\mathrm{d}\mu_{\mathrm{Cu}}}{\mathrm{d}T} = -\bar{S}^{\mathrm{Cu_2O}}_{\mathrm{Cu}} = -\frac{1}{2}S_{\mathrm{Cu_2O}} + \frac{1}{4}S^\circ_{\mathrm{O_2}} - \frac{1}{4}R\ln a_{\mathrm{O_2}} \tag{46}$$

Inserting Eq. (46) into Eq. (41) we find for the electrochemical potential gradient:

$$\left(\epsilon^{\mathrm{Cu_2O}}_{\mathrm{Cu}^+}\right)_{t\to\infty} = \frac{1}{F}\left(\frac{\mathrm{d}\tilde{\mu}_{\mathrm{Cu}^+}}{\mathrm{d}T}\right)_{\substack{t\to\infty \\ j\neq 0}} = -\frac{t_{\mathrm{Cu}^+}}{F}S^*_{\mathrm{Cu}^+} + \frac{t_{\mathrm{e}^-}}{F} \times\left(-\frac{1}{2}S_{\mathrm{Cu_2O}} + \frac{1}{4}S^\circ_{\mathrm{O_2}} - \frac{1}{4}R\ln a_{\mathrm{O_2}} + S^*_{\mathrm{e}^-}\right) \tag{47}$$

Inserting Eq. (47) into Eq. (7) we obtain the thermopower of the open cell in Eq. (12).

References

[1] D. Monceau, M. Filal, M. Tebtoub, C. Petot, G. Petot-Ervas, Solid State Ionics 73 (1994) 221–226.
[2] O. Teller, M. Martin, Solid State Ionics 101–103 (Pt. 1) (1997) 475–478.
[3] J.O. Hong, H.I. Yoo, Solid State Ionics 113–115 (1998) 265–270.
[4] J.O. Hong, H.I. Yoo, O. Teller, M. Martin, J. Mizusaki, Solid State Ionics 144 (2001) 241–248.
[5] I.V. Belova, M.J. Brown, G.E. Murch, Solid State Ionics 167 (2004) 175–182.
[6] H. Schmalzried, W. Laqua, P.L. Lin, Z. Naturforsch., A 34 (1979) 192–199.
[7] M. Martin, Mater. Sci. Rep. 7 (1991) 1–86.
[8] G. Petot-Ervas, C. Petot, D. Monceau, M. Loudjani, Solid State Ionics 53–56 (Pt. 1) 270–279.
[9] J.O. Hong, O. Teller, M. Martin, H.I. Yoo, Solid State Ionics 123 (1999) 75–85.
[10] D. Dimos, J. Wolfenstine, D.L. Kohlstedt, Acta Met. 36 (1988) 1543–1552.
[11] C. Reinke, W.C. Johnson, J. Am. Ceram. Soc. 78 (1995) 2593–2602.
[12] C. Sari, G. Schumacher, J. Nucl. Mater. 61 (1976) 192.
[13] F. Millot, P. Gerdanian, J. Nucl. Mater. 92 (1980) 257.
[14] W.T. Petuskey, H.K. Bowen, J. Am. Ceram. Soc. 64 (1981) 611.
[15] F. Millot, P. Gerdanian, J. Phys. Chem. Solids 43 (6) (1982) 501.
[16] F. Millot, P. Gerdanian, J. Nucl. Mater. 116 (1983) 55.
[17] H.-I. Yoo, J.H. Hwang, J. Phys. Chem. Solids 53 (1992) 973.
[18] D.-L. Kim, H.-I. Yoo, Solid State Ionics 81 (1995) 135.
[19] J. Janek, H. Timm, J. Nucl. Mater. 255 (1998) 116–127.
[20] H. Timm, Thermodiffusion in binären und ternären Oxiden, Dr. rer. nat. thesis, University of Hannover (1999).
[21] J. Janek, C. Korte, A.B. Lidiard, Thermodiffusion in ionic solids—model experiments and theory, in: W. Köhler, S. Wiegand (Eds.), Thermal Nonequilibrium Phenomena in Fluid Mixtures, Lecture Notes in Physics, Springer-Verlag, Berlin, 2002, pp. 146–183.
[22] A.R. Allnatt, A.V. Chadwick, Chem. Rev. 67 (1967) 681–705.
[23] A.R. Allnatt, A.B. Lidiard, Atomic Transport in Solids, Cambridge University Press, Cambridge, 1993.
[24] M. Yoshimura, A. Revcolevschi, J. Castaing, J. Mater. Sci. 11 (1976) 384–389.
[25] J. Xue, R. Dieckmann, J. Phys. Chem. Solids 51 (1990) 1263–1275.
[26] O. Porat, I. Riess, Solid State Ionics 74 (1994) 229–238.

[27] H. Duenwald, C. Wagner, Z. Phys. Chem., B 212–225 (1933).
[28] J. Gundermann, C. Wagner, Z. Phys. Chem., B 148–154 (1937).
[29] O. Porat, I. Riess, Solid State Ionics 81 (1995) 29–41.
[30] J. Maluenda, R. Farhi, G. Petot-Ervas, J. Phys. Chem. Solids 42 (1981) 697–699.
[31] N.L. Peterson, C.L. Wiley, J. Phys. Chem. Solids 45 (1985) 281–294.
[32] F. Perinet, J. Le Duigon, C. Monty, Non-stoichiometric compounds: surfaces, grain boundaries and structural Defects, NATO ASI Series C, vol. 276, 1989, pp. 387–397.
[33] C. Wagner, Prog. Solid State Chem. 7 (1972) 1–37.
[34] J. Janek, C. Korte, Z. Phys. Chem. 196 (1996) 187–208.
[35] J. Janek, C. Korte, Solid State Ionics 92 (1996) 193–204.
[36] D.R. Linde (Ed.), CRC Handbook of Chemistry and Physics, 75th ed., CRC Press, Boca Raton, 1994.
[37] O. Kubaschewski, C.B. Alcock, P.J. Spencer, Materials Thermochemistry, 6th ed., Pergamon Press, Oxford, 1993.
[38] F.L. Weichman, Phys. Rev. 117 (1960) 998.
[39] J. Dellacherie, B. Dalesdent, J. Rilling, J. Chim. Phys. 67 (1970) 360–367.
[40] F. Perinet, S. Barbezat, C. Monty, J. Phys., Colloq. C6 (1980) 315–318.
[41] J. Gundermann, C. Wagner, Z. Phys. Chem., B 155–156 (1937).
[42] C. Jones, P.J. Grout, A.B. Lidiard, Philos. Mag. Lett. 74 (1996) 217–223.
[43] C. Jones, P.J. Grout, A.B. Lidiard, Ber. Bunsenges. Phys. Chem. 101 (1997) 1232–1237.
[44] C. Jones, P.J. Grout, A.B. Lidiard, Philos. Mag., A 79 (1999) 2051–2070.
[45] M.J. Gillan, J. Phys. C. Solid State Phys. 10, 1641 (1977); 10, 3051 (1977).
[46] K. Wirtz, Phys. Z. 44 (1943) 221–231.
[47] J.A. Brinkman, Phys. Rev. 93 (1954) 345.
[48] A.D. LeClaire, Phys. Rev. 93 (1954) 344.
[49] G. Schottky, Phys. Status Solidi 8 (1965) 357–368.
[50] S. Miyatani, J. Phys. Soc. Jpn. 24 (1968) 328.
[51] T. Ohachi, T. Taniguchi, Solid State Ionics 3/4 (1981) 89.
[52] W. Koch, H. Rickert, G. Schlechtriemen, Solid State Ionics 9/10 (1983) 1197.
[53] A. Honders, E.W.H. Young, J.H.W. de Witt, G.H.J. Broers, Solid State Ionics 8 (1983) 115.
[54] A. Honders, A.J.H. Hintzen, J.M. der Kinderen, J.H.W. de Witt, G.H.J. Broers, Solid State Ionics 9/10 (1983) 1205.
[55] C. Korte, J. Janek, Z. Phys. Chem. 206 (1998) 129–163.
[56] J. Janek, C. Korte, Ber. Bunsenges. Phys. Chem. 99 (1995) 932–939.
[57] C. Korte, J. Janek, Ber. Bunsenges. Phys. Chem. 100 (1996) 425–432.
[58] C. Korte, J. Janek, J. Phys. Chem. Solids 58 (1997) 623–637.
[59] C. Korte, J. Janek, H. Timm, Solid State Ionics 101–103 (1997) 465–470.
[60] Hj. Matzke, J. Nucl. Mater. 30 (1987) 1121–1142.
[61] B.C.H. Steele, J.M. Floyd, Proc. Br. Ceram. Soc. 19 (1971) 55.
[62] B.A. van Hassel, B.A. Boukamp, A.J. Burggraaf, Solid State Ionics 48 (1991) 155.
[63] J. Corish, P.W.M. Jacobs, J. Phys. Chem. Solids 33 (1972) 179–1818.